



## Anticorrosion action of the olive leaf compounds extracted under optimal parameters as determined with experimental design

SOUAD TOUAZI<sup>1,2\*</sup>, MIHAEL M. BUČKO<sup>3#</sup>, RADOUANE MAIZIA<sup>2</sup>, SAMIRA SAHI<sup>1</sup>, NADIA ZAIDI<sup>2</sup> and LAID MAKHLOUFF<sup>2</sup>

<sup>1</sup>Laboratoire de Valorisation des Energies Fossiles (LAVALEF), Ecole Nationale Polytechnique d'Alger, Algeria, <sup>2</sup>Laboratoire d'Electrochimie, Corrosion et de Valorisation Energétique (LECVE), Faculté de Technologie, Université de Bejaia, Algeria and <sup>3</sup>Military Academy, University of Defence, Vojislava Lukića Kurjaka 33, Belgrade, Serbia

(Received 13 May, revised 6 July, accepted 1 August 2022)

**Abstract:** In this study, an agricultural waste product was used to prepare a green corrosion inhibitor based on olive leaves (*Olea europaea* var. *sysvestris*). Firstly, an optimization study of antioxidant activity of *O. europaea* leaves monitored by the DPPH free radical trapping method, was carried out using full factorial design. In the second step, the extract obtained under optimal conditions was tested as a green corrosion inhibitor for steel in 0.5 mol dm<sup>-3</sup> HCl, using gravimetric and electrochemical methods. The results obtained by various techniques showed that the extract acted as a mixed-type inhibitor. The adsorption of the inhibitor was spontaneous ( $\Delta G_{ads} = -12.443 \text{ kJ mol}^{-1}$ ), through the mechanism of physical adsorption, and it obeyed the Langmuir adsorption isotherm. The highest corrosion inhibition efficiency of 92 % was obtained for  $2.8 \cdot 10^{-3} \text{ g cm}^{-3}$  of inhibitor, as measured by gravimetric method.

**Keywords:** antioxidant activity; extraction; green inhibitor.

### INTRODUCTION

In industry, acid solutions are widely used, and the aggressiveness of these solutions causes metals degradation, either through chemical or electrochemical reactions. The most effective method of preventing or decreasing the bare metal dissolution in such acidic solutions, is the use of corrosion inhibitors, that are nowadays widely applied. Corrosion inhibitors are chemical compounds used to reduce the corrosion rate of metals and alloys in contact with aggressive environ-

\* Corresponding author. E-mail: souad.touazi@g.enp.edu.dz

# Serbian Chemical Society member.

<https://doi.org/10.2298/JSC220513064T>

ments at low concentrations,<sup>1</sup> thereby delaying and minimizing the corrosion process and thus avoiding economic losses due to metallic corrosion.

Numerous synthetic compounds show good corrosion inhibiting action, but many of them are extremely toxic to humans and environment. Therefore, the development of non-toxic and biodegradable corrosion inhibitors is becoming a key issue as new global guidelines for industrial discharges are becoming increasingly ecologically strict.<sup>2–6</sup> Plants are one of the sources for these inexpensive and clean inhibitors. Plant parts contain many compounds that satisfy the required criteria.

In the Mediterranean coastal zone, olive leaves are one of the by-products in the olive grove farming; they occur in high quantities in olive oil industry. They are also collected during the pruning of the olive trees.<sup>7</sup> Olive leaves are a cheap raw material known for its antioxidant properties.<sup>8</sup> Following this line, our work focuses on the inhibitory action of the olive leaf-based, green and natural substance, from *Olea europaea* var. *sylvestris*, in the corrosion process of steel in 0.5 mol dm<sup>-3</sup> HCl.

The present investigation was divided into two parts: in the first part, a full factorial design (FFD) optimization study of antioxidant activity of the extract from *O. europaea* leaves was conducted, using the DPPH free radical method. In the second part, the extract obtained under optimal conditions was tested for steel corrosion inhibition in hydrochloric acid by means of weight loss measurement, potentiodynamic polarization and impedance spectroscopy.

## EXPERIMENTAL

### Samples and reagents

Plant material consisting of leaves of *Olea europaea* var. *sylvestris* was harvested in the Algiers region, situated in the north of Algeria, during the flowering period between February and March 2018. The collected samples were identified by the national High School of Agronomy. The leaves were washed in distilled water, dried at room temperature, and subsequently dried in an oven at 40 °C. They were grounded to obtain the powder, and then stored in a closed plastic box.

Methanol, ethanol, 2,2-diphenyl-1-picrylhydrazyl (DPPH) and HCl (37 %) of analytical grade, were purchased from Sigma–Aldrich.

### Plant material extraction

The effects of different variables such as extraction temperature, solid/solvent ratio, water/ethanol ratio and extraction time, on the antioxidant activity, were studied using FFD. The conditions used in each experiment were settled according to the 2<sup>4</sup> FFD, as presented in Table I.

The powdered sample of *O. europaea*, which had been previously weighed, was placed in a Bicol flask, in contact with the extracting solvent. The mixture was kept in a thermostatic water bath with shaking. After a determined extraction time, the mixture was cooled in an ice bath, and then separated. The obtained filtered extracts were stored in the dark for future use

for the determination of their antioxidant activity. The concentration of extracts ( $\text{g cm}^{-3}$ ) was determined by evaporating  $10 \text{ cm}^3$  of the filtrate and then weighing the obtained residue.<sup>9</sup>

TABLE I. Range of coded and actual values for FF

Independent variable	Coded variable	Level		
		(-1)	(0)	(+1)
Extraction temperature, °C	$X_1$	55	68	81
Solid/solvent ratio, g $100 \text{ cm}^{-3}$	$X_2$	08	12	16
Water/ethanol ratio, vol. %	$X_3$	25	50	75
Extraction time, min	$X_4$	45	60	75

#### *Estimation of antioxidant activity*

The effect of each antioxidant on DPPH-radical was estimated according to the procedure described by Brand-Williams *et al.*<sup>10</sup> Briefly,  $1 \text{ cm}^3$  of the extract solution was added to  $9 \text{ cm}^3$  of DPPH ( $40 \mu\text{g cm}^{-3}$  prepared in methanol), and at the same time, a negative control (the blank) was prepared by mixing  $1 \text{ cm}^3$  of methanol with  $9 \text{ cm}^3$  of the methanol solution of DPPH. The samples were kept in the dark for 30 min. The absorbance measurements were carried out at the wavelength of 517 nm, using a UV–Vis spectrophotometer.

The antioxidant activity ( $AA / \%$ ) was calculated as:<sup>11</sup>

$$AA = (A_{\text{blank}} - A_{\text{sample}})/A_{\text{blank}} \quad (1)$$

where  $A_{\text{blank}}$  represents the absorbance of negative control and  $A_{\text{sample}}$  is the absorbance of the sample (diluted extract).

#### *Experimental design*

In this study, FFD methodology has been carried out to optimize the antioxidant activity of the samples. Two levels and four variables were used in this investigation, requiring 16 ( $2^4$ ) experiments plus four experiments performed at the center point to evaluate the experimental error variance. The four selected factors were studied between a lower level coded (-1), a higher level coded (+1) and the center point coded (0). The actual and coded levels of the independent variables are presented in Table I.

The regression equation which includes all interaction terms was given by the following expression:

$$Y_i = b_0 + \sum_{i=1}^4 b_i X_i + \sum_{i=3}^3 \sum_{j=i+1}^4 b_{ij} X_i X_j + \varepsilon \quad (2)$$

where  $Y_i$  is the predicted response,  $X_i$  represents the independent variables coded (1 or -1),  $b_0$  is the average value of the response of sixteen assays,  $b_i$  represents the principal effect, whereas  $b_{ij}$  represents the interaction effect and  $\varepsilon$  is a random error.

#### *Corrosion test*

The working electrode used in the present study was steel, with the chemical composition presented in Table II. Prior to each experiment, the working electrode was polished with various emery paper grades (280, 360, 800 and 1000), degreased with acetone and rinsed in distilled water before being placed into the aggressive solution.

For weight loss measurements, the steel coupons with a surface area of  $16.5 \text{ cm}^2$ , were immersed in  $100 \text{ cm}^3$  of  $0.5 \text{ mol dm}^{-3}$  HCl at  $25^\circ\text{C}$ , without and with different concentrations of the olive leaf extract. Corrosion rate ( $C_R$ ), inhibition efficiency ( $\eta$ ) and the degree of sur-

face coverage ( $\theta$ ) were calculated from the weight loss measurements, determined at different immersion times for a total duration of 8 days, by using the equations:<sup>12,13</sup>

$$C_R = (W_b - W_a)/A \quad (3)$$

$$\eta = 100(C_R(\text{free}) - C_R(\text{inh}))/C_R(\text{free}) \quad (4)$$

$$\theta = \eta/100 \quad (5)$$

where  $W_b$  and  $W_a$  are the coupon weight measured before and after immersion in the aggressive solution,  $A$  is the exposed area, and  $C_R(\text{free})$  and  $C_R(\text{inh})$  are the corrosion rates of steel in the absence and presence of the inhibitor in the aggressive solution, respectively.

TABLE II. Composition of steel

Element	C	Si	Mn	P	S	Mo	Fe
Content, wt. %	0.15–0.26	<0.35	<1.5	<0.035	<0.040	0.4–0.6	97–98

Open circuit potential (OCP) and potentiodynamic polarization measurements were carried out using a Voltamaster software piloted potentiostat PGZ100. This potentiostat was connected to the three electrodes: steel panel as a working electrode, a platinum panel used as a counter electrode and  $K_2SO_4$ -saturated sulphate electrode (SSE) as the reference.

Tafel plots were obtained at a scan rate of 1 mV s<sup>-1</sup>, over the respective OCP range between –250 and 250 mV (from cathodic to anodic end), after the constant OCP was established. The inhibition efficiency ( $\eta$ ) was determined as:<sup>14</sup>

$$\eta = 100(j_{\text{corr}}(\text{free}) - j_{\text{corr}}(\text{inh}))/j_{\text{corr}}(\text{free}) \quad (6)$$

where  $j_{\text{corr}}(\text{free})$  and  $j_{\text{corr}}(\text{inh})$  are the corrosion current densities in free and inhibited acid solution, respectively.

Electrochemical impedance spectroscopy (EIS) tests were carried out at OCP in an aerated solution using an Autolab potentiostat/galvanostat (PGSTAT30) under FRA software. The response of the electrochemical system to AC excitation was measured with a frequency ranging from 100 kHz to 10 mHz and peak to peak AC amplitude of 10 mV.

For the electrochemical tests, the exposed area of the steel was 1 cm<sup>2</sup>.

## RESULTS AND DISCUSSION

### *Optimization of extraction parameters*

Four variables and two levels were chosen to build the FFD in order to find the optimum combination of conditions for the extraction of active substances from the olive leaves. Variables such as extraction temperature ( $X_1$ ), solid/solvent ratio ( $X_2$ ), water/ethanol ratio ( $X_3$ ) and extraction time ( $X_4$ ) were selected as the independent variables, and antioxidant activity was taken as the response of the design experiments ( $Y$ ). The results collected to build the FFD model are given in Table S-I of Supplementary material to this paper.

To obtain the mathematical model that represents the antioxidant activity with the first order polynomial (Eq. (2)), the regression analysis was applied on the experimental data using Statistica Software 7.0. Various effects of factors and their interactions were calculated using the analysis of variance (ANOVA) and other adequacy measures.

Fig. 1 shows the Pareto chart, which represents the analysis of the calculated standardized effects of the independent variables and their interactions, on the response value of antioxidant activity. As can be seen in the Pareto charts, the solid/solvent ratio ( $X_2$ ) presented the most influencing parameter on the response. Whereas the interaction effects of extraction time with water/ethanol ratio ( $X_3, X_4$ ) and extraction time with solid/solvent ratio ( $X_2, X_4$ ) were insignificant, and therefore were eliminated from the regression equation. The negative value of the standardized effect indicates that the response decreases with increase of the value of this variable, and the opposite is the case for the positive value.

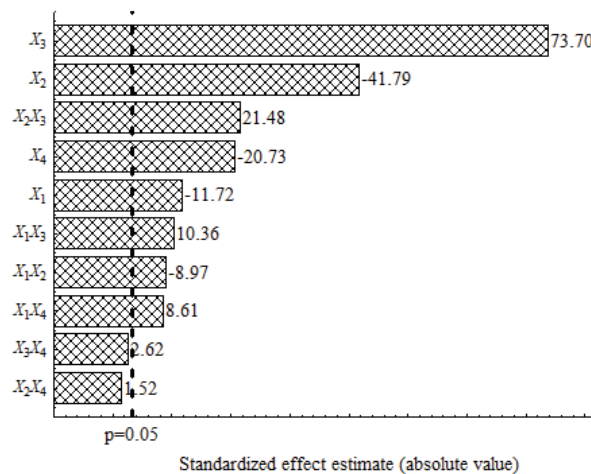


Fig. 1. Pareto chart of the response value of antioxidant activity on various independent variables and their interactions.

Table S-II of the Supplementary material shows the ANOVA analysis, used to verify the adequacy of the models at confidence level of 95 %. The regression  $p$ -value and  $F$ -value reveal that the model was highly significant and represented the data satisfactorily. In other words, the value of pure error is very low (0.84) suggesting strong data reproducibility.

A good adjustment of the regression equation to the experimental data was verified through the determination of coefficient value  $R^2$  (0.954) which is close to 1, indicating that only 4.6 % of the variations in observed data could not be explained by the model (Fig. 2a). The value of the adjusted  $R^2$  is equal to 0.905 which was also of very high importance to the model.

The comparison of experimental data and predicted values is shown in Fig. 2b. It can be seen that the predicted responses are in agreement with the experimental data and the difference between them does not exceed 0.055, indicating that the mathematical model is adequate. The final polynomial equation (Eq. (7))

representing the antioxidant activity as a function of the significant effects, was written as:

$$Y_i = 66.26 - 1.51X_1 + 9.73X_3 - 2.74X_4 - 1.18X_1X_2 + 1.73X_1X_3 + \\ + 1.14X_1X_4 + 2.83X_2X_3 \quad (7)$$

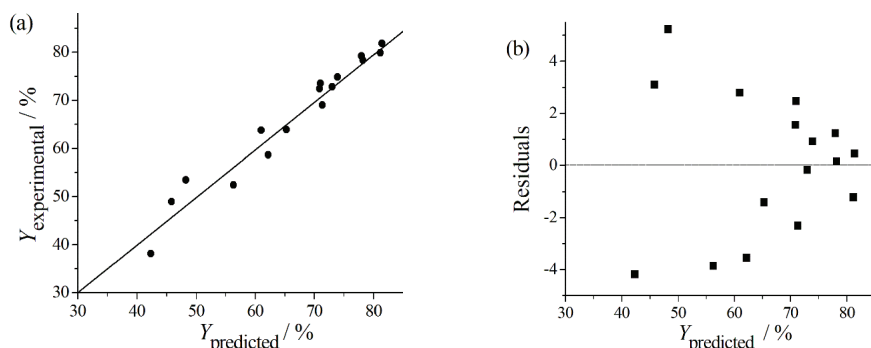


Fig. 2. Quality analysis of the model: a) experimental *versus* predicted responses, b) residual *versus* predicted value for antioxidant activity ( $Y_i$ ).

The numerical optimization of the desirability function gave optimal conditions to obtain olive leaf extract with a maximum antioxidant activity. With the analysis of the prediction profiler at maximal desirability (Fig. S-1 in the Supplementary material), it can be deduced that the best response of antioxidant activity was obtained at the following conditions: extraction temperature (55 °C), solid/solvent ratio (8 g 100 cm<sup>-3</sup>), water/ethanol ratio (75 %) and extraction time (45 min), with 0.99 as the value of desirability.

#### *Corrosion tests*

*Weight loss measurements.* Different concentrations of the olive leaf extract obtained under optimum conditions deduced from antioxidant capacity measurements, were added to 0.5 mol dm<sup>-3</sup> HCl. Corrosion of steel in the solutions prepared in this manner, was monitored by weight loss experiments, *i.e.*, by measuring the mass of the metal converted into corrosion products per unit of surface area, per unit of time. Fig. 3a and b represent the variation in corrosion rate and inhibitory efficiency, calculated from the weight loss measurements.

The Fig. 3 inspection shows clearly that the rate of steel corrosion is significantly reduced, *i.e.*, the inhibition efficiency is increased, with the addition of olive leaf extract. This behavior represents the extract's inhibiting effect against the acid corrosion of steel. The maximum inhibition efficiency of 92 % was achieved for 2.8 10<sup>-3</sup> g cm<sup>-3</sup> of the added extract.

*Open circuit potential measurements.* It is well known that the formation of protective corrosion products or a surface protective film in general, can be eva-

luted by monitoring the OCP of the corroding electrode. The effect of various concentrations of olive leaf extract on the steel electrode OCP in  $0.5 \text{ mol dm}^{-3}$  HCl, is shown in Fig. 4.

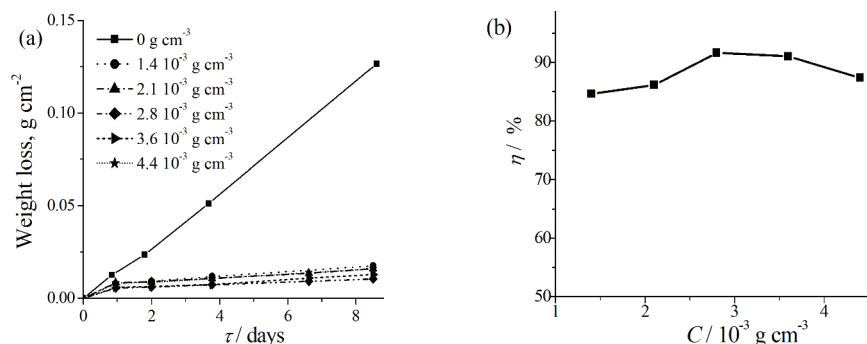


Fig. 3. a) Variation of the weight loss data with the immersion time recorded for steel electrode in  $0.5 \text{ mol dm}^{-3}$  HCl solution, in the absence and presence of various concentrations of extract; b) inhibition efficiency *versus* the concentration of the inhibitor, deduced from a).

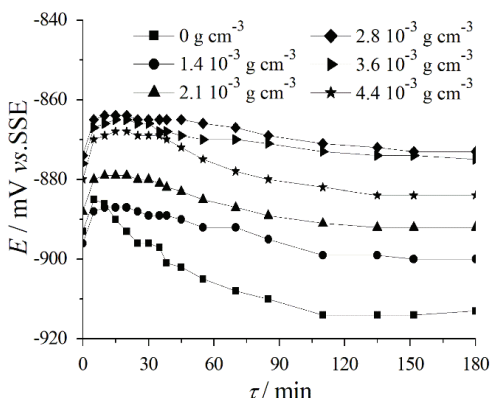


Fig. 4. OCP curves for steel in  $0.5 \text{ mol dm}^{-3}$  HCl solution as a function of time and inhibitor concentration.

The obtained results indicate that, as the immersion time increased, the OCP of the steel samples in the solution with the extract became more positive as compared to the OCP of the steel in the blank solution, which more rapidly shifted to negative values. The increase in the OCP, once the olive leaf extract was added, may be attributed to the adsorption of the inhibitor on the active metal sites.<sup>15</sup>

*Potentiodynamic polarization curves.* The inhibitive effect of olive leaf extract, on steel specimens immersed in  $0.5 \text{ mol dm}^{-3}$  HCl, was further studied by evaluating changes in cathodic and anodic behavior by recording the polarization curve from cathodic to anodic potential limit over the OCP at a scan rate of  $1 \text{ mV s}^{-1}$ .

Firstly, the effect of the extraction solvent (ethanol) on the typical anodic and cathodic polarization curves of steel in aggressive solution was studied as presented in Fig. 5a. The comparison of steel polarization in  $0.5 \text{ mol dm}^{-3}$  HCl blank solution and in  $0.5 \text{ mol dm}^{-3}$  HCl with ethanol, does not indicate any influence of ethanol. Therefore, the strong inhibitory activity of the extract observed at Tafel plots in Fig. 5b is primarily due to the presence of olive leaf compounds.

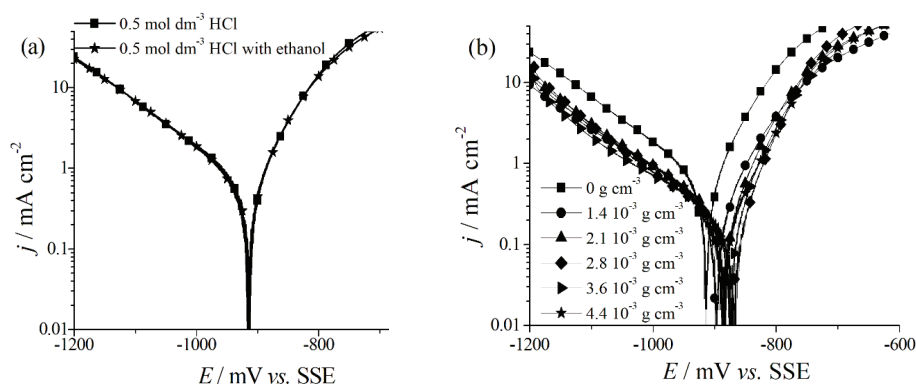


Fig. 5. Potentiodynamic polarization of steel in  $0.5 \text{ mol dm}^{-3}$  HCl blank solution and in the presence of: a) ethanol; b) different concentrations of olive leaf extract.

Steel corrosion parameters determined from polarization curves in  $0.5 \text{ mol dm}^{-3}$  HCl blank solution and in the solution containing olive leaves extract, are shown in Table III. Inspection of the obtained results revealed that the values of corrosion potential ( $E_{\text{corr}}$ ) and corrosion current density ( $j_{\text{corr}}$ ) were influenced by the presence of the inhibitor. As shown in Fig. 5b, the increase in the extract concentration results in lower current densities recorded from the potentiostatic polarization curves. Besides, the  $E_{\text{corr}}$  slightly shifts to a more positive value (noble direction of potential) in the presence of olive leaf extract.

TABLE III. Electrochemical parameters obtained from polarization curves at  $25^\circ\text{C}$ .

$C / \text{mg cm}^{-3}$	$E_{\text{corr}} / \text{mV vs.SSE}$	$j_{\text{corr}} / \text{mA cm}^{-2}$	$b_a / \text{mV dec}^{-1}$	$b_c / \text{mV dec}^{-1}$	$\eta / \%$
0	-932	1.13	65	143	—
1.4	-905	0.48	39	266	57.5
2.1	-898	0.40	58	159	64.6
2.8	-882	0.22	56	151	80.5
3.6	-884	0.29	63	166	74.3
4.4	-890	0.30	63	156	73.4

Since the difference between the  $E_{\text{corr}}$  of the steel electrode in the blank solution and in the solution containing inhibitor is lower than  $85 \text{ mV}$ , this behavior suggests that the extract functions as a mixed-type inhibitor.<sup>16,17</sup>

The highest inhibition efficiency of 80.53 % was obtained for the extract concentration value of  $2.8 \times 10^{-3}$  g cm<sup>-3</sup>. As can be seen, the inhibition efficiency, both determined by gravimetric tests (Fig. 3) and polarization curves (Table III), increases with increasing the olive leaf extract concentration until reaching a peak value at optimal extract concentration.

The values of inhibition efficiency calculated by gravimetric measurements were higher than those calculated by the electrochemical method. A similar finding between the two approaches has previously been recorded.<sup>18</sup> The disparity observed may be due to the fact that the gravimetric method provides average corrosion rates, while electrochemical techniques give instantaneous corrosion rates. Indeed, the development of a protective film during the immersion time of 8 days, in the case of gravimetric measurement, may explain the difference between the obtained values.

*Adsorption isotherms.* The adsorption of the olive leaf extract compounds at the steel surface is assumed to be responsible for the inhibitory action of the extract against the corrosion of steel in acid solution. The adsorbed layer functions as a barrier between the steel surface and the aggressive solution, resulting in a reduction of the rate of corrosion.<sup>19</sup> Consequently, the inhibition efficiency ( $\eta$ ) derived from the weight loss curves is directly proportional to the fraction of the surface covered by the adsorbed molecules ( $\theta$ ).<sup>20</sup> The mode of variation of ( $\theta$ ) with the extract concentration ( $C$ ) determines the adsorption isotherm describing the system.<sup>21</sup> Several adsorption isotherms (Langmuir, Temkin and Frumkin) were evaluated to determine the effective adsorption isotherm, according to the following equations:<sup>22,23</sup>

$$\text{Langmuir: } C/\theta = 1/K + C \quad (8)$$

$$\text{Temkin: } e^{-2\alpha\theta} = KC \quad (9)$$

$$\text{Frumkin: } \frac{\theta}{1-\theta} e^{-2\alpha\theta} = KC \quad (10)$$

where  $\alpha$  is the adsorbate interaction parameter and  $K$  the equilibrium constant of the adsorption process (L kg<sup>-1</sup>), related to the adsorption free energy change ( $\Delta G_{\text{ads}}^0$ ) by the following equation:

$$\Delta G_{\text{ads}}^0 = -RT \ln(55.5K) \quad (11)$$

where  $R$  is the gas constant (J °K<sup>-1</sup>mol<sup>-1</sup>) and  $T$  the temperature (K).

According to the experimental data, the relationship of ( $\theta$ ) versus  $C$  was observed to follow a linear pattern (Fig. 6), which can be described by Langmuir equation (Eq. (8)) with  $R^2$ -value equal to 0.99. The other equations (Eqs. (9) and (10)) were evaluated but did not indicate a good fit (for Temkin and Frumkin isotherms, the  $R^2$ -values obtained were 0.37 and 0.005 respectively).

The calculated values of adsorption equilibrium constant ( $K$ ) and free energy change of adsorption ( $\Delta G_{\text{ads}}^0$ ) were found to be 2.73 L kg<sup>-1</sup> and -12.443 kJ

$\text{mol}^{-1}$ , respectively. The negative sign shows that the adsorption of olive leaf extract onto steel surface is a spontaneous process. The values of  $\Delta G^0_{\text{ads}}$  of  $-20 \text{ kJ mol}^{-1}$  or more positive, are well known to suggest physical adsorption, while values of  $-40 \text{ kJ mol}^{-1}$  or more negative, involve charge sharing, *i.e.*, the charge transfer from the inhibitor molecules to the metal surface, to form the chemisorption related coordinate type of bond.<sup>9,24</sup> The acquired value of  $\Delta G^0_{\text{ads}}$  in our work shows a strong physical adsorption of the olive leaf extract components onto the steel surface in  $0.5 \text{ mol dm}^{-3}$  HCl solution.

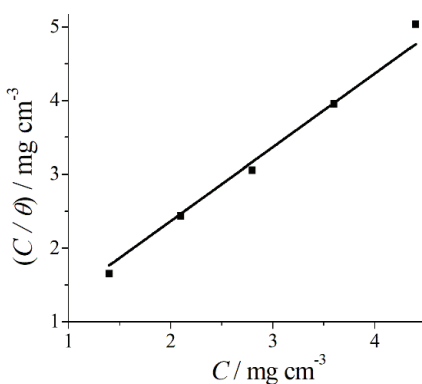


Fig. 6. Langmuir isotherm for adsorption of olive leaf extract onto steel surface in  $0.5 \text{ mol dm}^{-3}$  HCl solution at  $25^\circ\text{C}$ .  $R^2 = 0.99$ .

**Electrochemical impedance spectroscopy.** The electrochemical impedance spectroscopy is used as a powerful technique to characterize the corrosion parameters at metal/electrolyte interface. Fig. 7 highlights the Nyquist plots of steel samples immersed in  $0.5 \text{ mol dm}^{-3}$  HCl solution in the absence and presence of various concentrations of the olive leaf extract at the OCP. The impedance plots obtained are similar in shape and consist of a single capacitive semicircle at high-to-medium frequency and an inductive loop at low frequency range. The capacitive loop is related to the charge transfer resistance process, while the appearance of the pseudo-inductive loop can be explained by the relaxation of adsorption species such as  $(\text{Cl}^-)_{\text{ads}}$  and  $(\text{H}^+)_{\text{ads}}$  on the surface of the electrode.<sup>25</sup> The inductive loop can also be related to the re-dissolution of the passivated surface.<sup>26,27</sup> Also, one can see that the addition of the olive leaf extract inhibitor, increases the size of the semi-circle in comparison to the blank solution, and the maximum circle diameter is obtained for  $2.8 \times 10^{-3} \text{ g cm}^{-3}$  of inhibitor. This shows that there is an increase in the charge transfer resistance, which is in agreement with the literature,<sup>25,26,28</sup> and previous corrosion tests in this work. The improvement in the resistance by increasing the inhibitor concentration is due to an adsorption of inhibitor molecules on the surface of the steel, indicating the effective blocking of the surface.<sup>29</sup>

The impedance data were analyzed using ZSimpWin® software and fitted to the equivalent circuit model shown in Fig. 8. This equivalent circuit is exten-

sively reported in the literature.<sup>30,31</sup> The elements related to the circuit are:  $R_e$  representing the electrolyte resistance,  $R_{ct}$  as the charge transfer resistance,  $L$  as the inductance element,  $R_L$  as an inductive resistance,  $Q$  as the pseudocapacitance and CPE as the constant phase element.

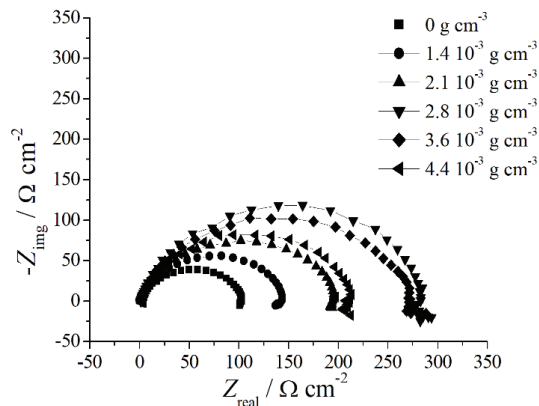


Fig. 7. Nyquist plots for mild steel in  $0.5\text{ mol dm}^{-3}$  HCl solution in the absence and presence of olive leaf extract at  $E_{corr}$  and  $T = 25^\circ\text{C}$ .

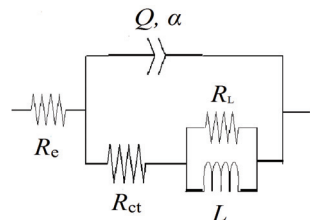


Fig. 8. Electrical equivalent circuit model used to fit the impedance parameters for steel electrode in  $0.5\text{ mol dm}^{-3}$  HCl solution.

Due to the roughness and homogeneity of the metal surface, as well as adsorption effects, CPE can be used to replace the double-layer capacitance,  $C_{dl}$ .<sup>26</sup> The electrochemical impedance parameters obtained from the equivalent circuit are presented in Table IV.

TABLE IV. EIS parameters for the corrosion of steel immersed in  $0.5\text{ mol dm}^{-3}$  HCl without and with different concentrations of olive leaf extract

$C/\text{mg cm}^{-3}$	$R_e/\Omega \text{m}^2$	$Q/10^{-5}\Omega^{-1}s^n\text{cm}^{-2}$	$n$	$R_{ct}/\Omega \text{cm}^2$	$R_L/\Omega \text{cm}^2$	$L/\text{H cm}^2$
0	1.14	36.64	0.80	99.22	6.63	9.20
1.4	0.87	29.69	0.82	135.50	13.37	16.77
2.1	1.23	25.33	0.81	187.20	14.01	32.95
2.8	0.96	26.41	0.84	247.50	45.44	377.70
3.6	0.95	28.93	0.82	218.30	56.11	1552
4.4	1.44	20.48	0.87	208.20	$2.37 \times 10^{10}$	0.10

From Table IV, a significant increase in the charge transfer resistance ( $R_{ct}$ ) was observed in the presence of the inhibitor, providing a high anticorrosive efficiency. The largest effect was observed at  $2.8 \times 10^{-3}\text{ g cm}^{-3}$  of olive leaf extract,

which gave  $R_{ct}$  value equal to  $247 \Omega \text{ cm}^2$ . This behavior is due to an adsorption of inhibitor molecules on the metal surface, leaving less electroactive sites available for corrosion, *i.e.*, the inhibitor builds up a protective film on the metallic surface that isolates it from the corrosive environment, thereby impeding further charge and mass transfer.<sup>31,32</sup>

In addition, the increased  $n$  value after the addition of extract to the hydrochloric acid solution (0.82–0.87) when compared to that obtained in the blank solution (0.80), indicates the reduction in the surface in homogeneity due to the adsorption of inhibitor molecules on the active adsorption sites at steel surface.<sup>32,33</sup> Also, from Table IV, one can notice that the  $Q$  value is lower in the presence of olive leaf extract compared to the blank solution. The diminishing values of  $Q$  can be related to a lower local dielectric constant due to the replacement of water molecules with inhibitor molecules. This process increases the thickness of the electrical double layer and reduces the surface area exposed to the aggressive media, implying an adsorption of inhibitor molecules on the surface of the steel.<sup>31,32</sup>

#### CONCLUSION

In the present work, an optimization study of the antioxidative matter extraction from *Olea europaea* var. *sylvestris* leaves was performed using full factorial design. The statistical analysis of the experimental results showed that the final polynomial equation, representing the antioxidant activity as a function of the significant effect, gave a reasonably good fit with an  $R^2$  value of 0.955. By response optimizer graph plot, the best response value of antioxidant activity was acquired at the following extraction parameters: extraction temperature 55 °C, solid/solvent ratio 8 g 100 cm<sup>-3</sup>, water/ethanol ratio 75 %, and extraction time 45 min.

Afterwards, the olive leaf extract obtained under the final optimized conditions was tested as a green corrosion inhibitor for steel in 0.5 mol dm<sup>-3</sup> HCl. Results of the electrochemical performance and weight loss analysis of steel samples, in HCl with the addition of *O. europaea* leaf extract, indicated that the extract:

- is a successful corrosion inhibitor for steel in 0.5 mol dm<sup>-3</sup> HCl solution, with a maximum inhibition efficiency of 92 %, achieved at extract concentration of  $2.8 \times 10^{-3}$  g cm<sup>-3</sup>,
- acts as a mixed-type inhibitor and
- acts as an adsorption inhibitor, where the adsorption phenomenon is spontaneous, following the mechanism of physical adsorption related to the Langmuir adsorption isotherm.

## SUPPLEMENTARY MATERIAL

Additional data and information are available electronically at the pages of journal website: <https://www.shd-pub.org.rs/index.php/JSCS/article/view/11851>, or from the corresponding author on request.

## ИЗВОД

**АНТИКОРОЗИОНО ДЕЈСТВО СУПСТАНЦИ ЕКСТРАХОВАНИХ ИЗ ЛИШЋА МАСЛИНЕ  
ПОД ОПТИМАЛНИМ ПАРАМЕТРИМА, ПРЕТХОДНО ОДРЕЂЕНИМ ПРИМЕНОМ  
МЕТОДОЛОГИЈЕ EXPERIMENTAL DESIGN**

SOUAD TOUAZI<sup>1,2</sup>, МИХАЕЛ М. БУЧКО<sup>3</sup>, RADOUANE MAIZIA<sup>2</sup>, SAMIRA SAHI<sup>1</sup>, NADIA ZAIDI<sup>2</sup>  
и LAID MAKHLOUFI<sup>2</sup>

<sup>1</sup>Laboratoire de Valorisation des Energies Fossiles (LAVALEF), Ecole Nationale Polytechnique d'Alger, Algeria,

<sup>2</sup>Laboratoire d'Electrochimie, Corrosion et de Valorisation Energétique (LECVE), Faculté de Technologie,

Université de Bejaia, Algeria и <sup>3</sup>Војна академија, Универзитет одбране,

Вељка Лукића Курјака 33, Београд

У овом истраживању, лишће маслине (*Olea europaea* var. *sylvestris*) је искоришћено за добијање зеленог инхибитора корозије. Прво су одређени оптимални параметри екстракције активних материја из лишћа, мерењем њихове антиоксидантне активности на слободним органским радикалима. Оптимизација параметара је извршена *full factorial design* методом. У другој фази истраживања, екстракт добијен при оптималним параметрима је испитиван као инхибитор корозије челика у 0,5 mol dm<sup>-3</sup> HCl, гравиметријском и електрохемијским методама. Резултати показују да се екстракт понаша као мешовити инхибитор. Адсорпција инхибитора на супстрату је спонтана ( $\Delta G_{ads}^0 = -12,443 \text{ kJ mol}^{-1}$ ), одиграва се према механизму физичке адсорпције и може се описати Лангмировом адсорpcionом изотермом. Највећи степен инхибиирања корозије од 92 % мерено гравиметријском методом, се постиже при концентрацији инхибитора у киселини од  $2,8 \times 10^{-3} \text{ g cm}^{-3}$ .

(Примљено 13. маја, ревидирано 6. јула, прихваћено 1. августа 2022)

## REFERENCES

1. D. Bouknana, B. Hammouti, H. Serghini Caid, S. Jodeh, A. Bouyanzer, A. Aouniti, I. Warad, *Int. J. Ind. Chem.* **6** (2015) 233 (<http://dx.doi.org/10.1007/s40090-015-0042-z>)
2. A. Y. El-Etre, M. Abdallah, Z. E. El-Tantawy, *Corros. Sci.* **47** (2005) 385 (<http://dx.doi.org/10.1016/j.corsci.2004.06.006>)
3. A. Zaabar, R. Aitout, D. Amoura, R. Maizia, L. Makhloufi, B. Saidani, *Miner. Eng.* **142** (2019) 105 (<http://dx.doi.org/10.1016/j.jcrusgro.2013.09.048>)
4. A. Zaabar, R. Aitout, L. Makhloufi, K. Alilat, S. Maziz, B. Saidani, *Hydrometallurgy* **136** (2013) 58 (<http://dx.doi.org/10.1016/j.hydromet.2013.03.004>)
5. G. Salinas-Solano, J. Porcayo-Calderon, A. K. Larios-Galvez, J. G. Gonzalez-Rodriguez, *J. Electrochem. Sci. Eng.* **12** (2022) 373 (<https://doi.org/10.5599/jese.1017>)
6. S. E. Adeniji, B. A. Akindehinde, *J. Electrochem. Sci. Eng.* **8** (2018) 219 (<https://doi.org/10.5599/jese.486>)
7. J. Tabera, A. Guinda, A. Ruiz-Rodriguez, F. J. Senorans and E. Ibanez, *J. Agr. Food. Chem.* **52** (2004) 4774 ([http://dx.doi.org/10.1021/jf049881+\)](http://dx.doi.org/10.1021/jf049881+)
8. R. Briante, M. Patumi, S. Terenziani, E. Bismuto, F. Febbraio, *J. Agr. Food. Chem.* **50** (2002) 4934 (<http://dx.doi.org/10.1021/jf025540p>)
9. A. Zaabar, R. Aitout, L. Makhloufi, K. Belhamel, B. Saidani, *Pigment Resin Technol.* **43** (2014) 127 (<http://dx.doi.org/10.1108/PRT-11-2012-0078>)

10. W. Brand-Williams, M. E. Cuvelier, C. Berset, *Lwt-Food. Sci. Technol.* **28** (1995) 25 ([http://dx.doi.org/10.1016/S0023-6438\(95\)80008-5](http://dx.doi.org/10.1016/S0023-6438(95)80008-5))
11. Y. Carmona-Jiménez, M. V. García-Moreno, J. M. Igartuburu, C. G. Barroso, *Food Chem.* **165** (2014) 198 (<http://dx.doi.org/10.1016/j.foodchem.2014.05.106>)
12. A. A. Rahim, E. Rocca, J. M. Steinmetz, J. Kassim, R. Adnan, M. S. Ibrahim, *Corros. Sci.* **49** (2007) 402 (<http://dx.doi.org/10.1016/j.corsci.2006.04.013>)
13. N. A. Negm, N. G. Kandile, A. E. Badr, M. A. Mohammed, *Corros. Sci.* **65** (2012) 94 (<http://dx.doi.org/10.1016/j.corsci.2012.08.002>)
14. A. Y. El-Etre, *J. Colloid Interface Sci.* **314** (2007) 578 (<http://dx.doi.org/10.1016/j.jcis.2007.05.077>)
15. M. Keramatinia, B. Ramezanzadeh, M. Mahdavian, *J. Taiwan Inst. Chem. Eng.* **105** (2019) 134 (<http://dx.doi.org/10.1016/j.jtice.2019.10.005>)
16. N. Soltani, N. Tavakkoli, M. Khayatkashani, M. R. Jalali, A. Mosavizade, *Corros. Sci.* **62** (2012) 122 (<http://dx.doi.org/10.1016/j.corsci.2012.05.003>)
17. J. N. Asegbeloyin, P. M. Ejikeme, L. O. Olasunkanmi, A. S. Adekunle, E. E. Ebenso, *Materials* **8** (2015) 2918 (<http://dx.doi.org/10.3390/ma8062918>)
18. A. M. Al-Turkustani, S. T. Arab, L. S. S. Al-Qarni, *J. Saudi Chem. Soc.* **15** (2011) 73 (<http://dx.doi.org/10.1016/j.jschs.2010.10.008>)
19. M. A. Bidia, M. Azadia, M. Rassouli, Mater. *Today Commun.* **24** (2020) 100996 (<http://dx.doi.org/10.1016/j.mtcomm.2020.100996>)
20. R. Farahatia, S. M. Mousavi-Khoshdela, *Prog. Org. Coat.* **142** (2020) 105567 (<http://dx.doi.org/10.1016/j.porgcoat.2020.105567>)
21. Z. Bajić, D. Pamučar, J. Bogdanov, M. Bučko, Z. Veličković, *Milit. Tech. Courier* **67** (2019) 735 (<http://dx.doi.org/10.5937/vojtehg67-21519>)
22. A. Fateh, M. Aliofkhazraei, A. R. Rezvanian, *Arab. J. Chem.* **13** (2020) 481 (<http://dx.doi.org/10.1016/j.arabjc.2017.05.021>)
23. N.K. Gupta, C. Verma, R. Salghi, H. Lgaz, A. K. Mukherjee, M. A. Quraishi, *New J. Chem.* **41** (2017) 13114 (<http://dx.doi.org/10.1039/C7NJ01431G>)
24. A. K. Singh, M. A. Quraishi, *Corros. Sci.* **53** (2011) 1288 (<http://dx.doi.org/10.1016/j.corsci.2011.01.002>)
25. E. de B. Pollicarpio, A. Spinelli, J. Taiwan. *Inst. Chem. Eng.* **116** (2020) 215 (<http://dx.doi.org/10.1016/j.jtice.2020.10.024>)
26. T. Rabizadeh, S. K. Asl, *J. Mol. Liq.* **276** (2019) 694 (<http://dx.doi.org/10.1016/j.molliq.2018.11.162>)
27. H. Ashassi-Sorkhabi, E. Asghari, *Electrochim. Acta* **54** (2008) 162 (<http://dx.doi.org/10.1016/j.electacta.2008.08.024>)
28. F. E. Abeng, V. Anadebe, P. Y. Nkom, K. J. Uwakwe, E. G. Kamalu, *J. Electrochem. Sci. Eng.* **11** (2022) 11 (<https://doi.org/10.5599/jese.1017>)
29. M. A. Chidiebere, E. E. Oguzie, L. Liu, Y. Li, F. Wang, *J. Ind. Eng. Chem.* **26** (2015) 182 (<http://dx.doi.org/10.1016/j.jiec.2014.11.029>)
30. I. Danaee, P. Nikparsa, M. R. Khosravi-Nikou, H. Eskandari, S. Nikmanesh, *Prot. Met. Phys. Chem. Surf.* **55** (2019) 1001 (<http://dx.doi.org/10.1134/S2070205119050289>)
31. A. Sedik, D. Lerari, A. Salci, S. Athmani, K. Bachari, I.H. Gecibesler, R. Solmaz, *J. Taiwan Inst. Chem. Eng.* **107** (2020) 189 (<http://dx.doi.org/10.1016/j.jtice.2019.12.006>)
32. P. Mourya, S. Banerjee, M. M. Singh, *Corros. Sci.* **85** (2014) 352 (<http://dx.doi.org/10.1016/j.corsci.2014.04.036>)
33. H. Zarrok, A. Zarrouk, B. Hammouti, R. Salghi, C. Jama, F. Bentiss, *Corros. Sci.* **64** (2012) 243 (<http://dx.doi.org/10.1016/j.corsci.2012.07.018>).